J. Austral. Math. Soc. Ser. B 33(1991), 240–253

GROUND MOTION ON ALLUVIAL VALLEYS UNDER INCIDENT PLANE SH WAVES

DAVID L. CLEMENTS and ASHLEY LARSSON[1]

(Received 10 August 1990)

Abstract

The scattering and diffraction of harmonic SH waves by an arbitrarily shaped alluvial valley in a layered material is considered. The problem is solved in terms of boundary integral equations which yield a numerical solution.

1. Introduction

After a substantial earthquake it is often found that damage is concentrated in particular areas [5]. This may be accounted for by various causes such as poor quality of construction, local topography and the local geology. One explanation which has been put forward is that the damage distribution is caused by seismic wave amplification associated with the local topography and soil characteristics [10].

Motivated by the need to provide reliable design parameters for structures, the problem has been studied by numerous authors. In certain circumstances ground-motion amplifications can be studied adequately by simple shear-beam amplification models. However, for irregular topographies, the problem must be studied as a spatial phenomenon. The simplest models which yield significant information in this area are two-dimensional, and several studies ([1], [2], [3], [7], [8], [10]) of this type have provided a basic understanding of the problem.

Integral equation formulations have been found to be particularly useful in obtaining numerical solutions to problems of this type. In particular, Wong and Jennings [9] used singular integral equations to solve the problem of

[1]Department of Applied Mathematics, University of Adelaide, South Australia, 5000.

scattering and diffraction of SH-waves by canyons of arbitrary cross section. Subsequently Wong et al. [11] extended the method of [9] to the case of a layer overlying a semi-infinite soil medium, and applied their analysis to modeling the variations in measured displacements during a full-scale low-amplitude wave propagation test. Also Sanchez-Sesma and Esquivel [6] considered ground motion on alluvial valleys under incident planar SH-waves.

The present work can be considered as an extension of previous work on integral equation formulations to include the case of anisotropic materials. In many cases the medium through which the waves are propagating is not homogeneous and isotropic, and is more accurately modeled as an anisotropic material. In particular, the current work examines the effect of anisotropy on ground motion on alluvial valleys under incident planar SH waves. Numerical results are obtained, and these are compared with those given in [6] for isotropic materials.

2. Statement of the problem

Referring to a Cartesian frame $Ox_1x_2x_3$, consider an anisotropic elastic half-space occupying the region $x_2 > 0$. The half-space is divided into two regions which contain different homogeneous anisotropic materials (see Figure 1). The materials are assumed to adhere rigidly to each other so that the displacement and stress are continuous across the interface. Also, the geometries of the two regions are assumed not to vary in the Ox_2 direction, and the boundary $x_2 = 0$ is traction free.

A horizontally polarised SH wave propagates towards the surface of the elastic half-space. This is in the form of a plane wave with unit amplitude,

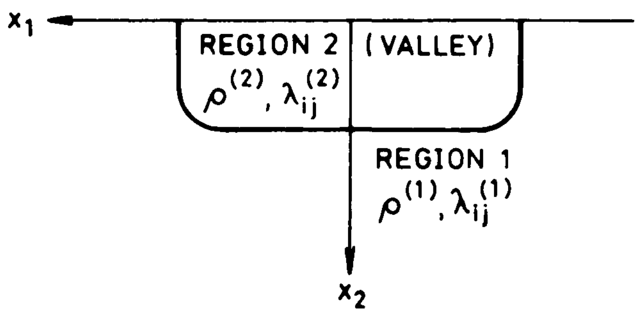

FIGURE 1. The alluvial valley and surrounding half-space.

https://doi.org/10.1017/S0334270000007013 Published online by Cambridge University Press

and gives rise to a displacement field

$$u_{3I}^{(1)} = \exp i\omega\left(t + \frac{x_1}{c_1} + \frac{x_2}{c_2}\right) \tag{1}$$

where ω is the circular frequency, c_1 and c_2 are constants and $u_3^{(1)}$ denotes the displacement in the Ox_3 direction in region 1 (see Figure 1). The problem is to determine the displacements associated with the reflected, diffracted and refracted waves.

3. Integral equation formulation

Since the incident wave is of the form (1), and the geometry does not vary in the Ox_3 direction, a solution of the problem can be obtained in terms of plane polarised SH waves. For such waves, the only nonzero displacement in this case is u_3, which must satisfy the equation of motion for antiplane elastic deformations of anisotropic materials. That is,

$$\lambda_{ij}^{(\alpha)}\frac{\partial^2 u_3^{(\alpha)}}{\partial x_i \partial x_j} = \rho^{(\alpha)}\frac{\partial^2 u_3^{(\alpha)}}{\partial t^2} \quad \text{for } \alpha = 1\,,2 \tag{2}$$

where $u_3^{(1)}$ and $u_3^{(2)}$ denote the displacements in regions 1 and 2 respectively. Also $\lambda_{ij}^{(\alpha)}$ denote the elastic moduli, which must satisfy the symmetry conditions $\lambda_{ij}^{(\alpha)} = \lambda_{ji}^{(\alpha)}$, $\rho^{(\alpha)}$ denotes the density, t denotes the time, and summation from 1 to 2 is assumed for repeated Latin indices only.

In view of the form of the incident plane wave (1), a solution to (2) is sought for which the displacement has a time dependence of the form $\exp(i\omega t)$ so that

$$u_3^{(\alpha)}(x_1\,, x_2\,, t) = u^{(\alpha)}(x_1\,, x_2)\exp(i\omega t)\,. \tag{8}$$

Equation (3) provides a solution to (2) if $u^{(\alpha)}$ satisfies the equation

$$\lambda_{ij}^{(\alpha)}\frac{\partial^2 u^{(\alpha)}}{\partial x_i \partial x_j} + \rho^{(\alpha)}\omega^2 u^{(\alpha)} = 0\,. \tag{4}$$

Suppose the incident wave (1) has an angle of incidence γ_I (Figure 2). Then $c_1 = \beta^{(1)}/\sin\gamma_I$ and $c_2 = \beta^{(1)}/\cos\gamma_I$ where $\beta^{(1)}$ is a constant. Now $u_3^{(1)}$ as given by (1) must satisfy (2) so that

$$[\beta^{(1)}]^2 = \frac{\lambda_{11}^{(1)}\sin^2\gamma_I + 2\lambda_{12}^{(1)}\sin\gamma_I\cos\gamma_I + \lambda_{22}^{(1)}\cos^2\gamma_I}{\rho^{(1)}} \tag{5}$$

where $\beta^{(1)}$ is the wave velocity of the incident wave.

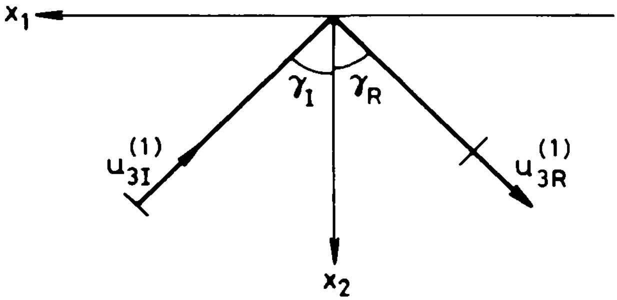

FIGURE 2. Angles of incidence and reflection.

Consider the case when regions 1 and 2 are occupied by the same material. In order to satisfy the traction-free surface condition on $x_2 = 0$, it is necessary to have a reflected wave of the form

$$u_{3R}^{(1)} = \exp i\omega \left(t + \frac{x_1}{c_1'} - \frac{x_2}{c_2'} \right) . \tag{6}$$

The displacement $u_{3R}^{(1)}$ in the half-space is given by the sum of the displacements given by (1) and (6). Thus

$$u_3^{(1)} = u_{3R}^{(1)} = \exp i\omega \left(t + \frac{x_1}{c_1} + \frac{x_2}{c_2} \right) + \exp i\omega \left(t + \frac{x_1}{c_1'} - \frac{x_2}{c_2'} \right) . \tag{7}$$

The stresses are given by

$$\sigma_{i3}^{(\alpha)} = \lambda_{ij}^{(\alpha)} \frac{\partial u_3^{(\alpha)}}{\partial x_j} \tag{8}$$

so that the stress $\sigma_{23}^{(1)}$ on $x_2 = 0$ is

$$\sigma_{23}^{(1)} = \left(\frac{\lambda_{21}^{(1)}}{c_1'} - \frac{\lambda_{22}^{(1)}}{c_2'} \right) \exp \left[i\omega \left(t + \frac{x_1}{c_1'} \right) \right] + \left(\frac{\lambda_{21}^{(1)}}{c_1} + \frac{\lambda_{22}^{(1)}}{c_2} \right) \exp \left[i\omega \left(t + \frac{x_1}{c_1} \right) \right] . \tag{9}$$

This stress will be zero for all time t if

$$c_1' = c_1$$

and

$$-\frac{\lambda_{21}^{(1)}}{c_1} + \frac{\lambda_{22}^{(1)}}{c_2'} = \frac{\lambda_{21}^{(1)}}{c_1} + \frac{\lambda_{22}^{(1)}}{c_2}$$

or

$$\frac{1}{c_2'} = \frac{1}{c_2} + \frac{2\lambda_{21}^{(1)}}{\lambda_{22}^{(1)} c_1} . \tag{10}$$

https://doi.org/10.1017/S0334270000007013 Published online by Cambridge University Press

This equation serves to provide c_2' in terms of the unknown quantities c_2, c_1, $\lambda_{21}^{(1)}$ and $\lambda_{22}^{(1)}$. Note that if (6) is substituted into (2) then since it represents a solution to (2) it follows that

$$\frac{\lambda_{11}^{(1)}}{c_1^2} - \frac{2\lambda_{12}^{(1)}}{c_1 c_2'} + \frac{\lambda_{22}^{(1)}}{c_2'^2} = \rho^{(1)} \tag{11}$$

and if (10) is used to substitute for $1/c_2'$ in (11), and then into (5), so that (10) ensures (6) is a solution to (2) on the assumption that (1) is also a solution to (2).

Let $c_1 = \beta'/\sin(\gamma_R)$ and $c_2' = \beta'/\cos(\gamma_R)$ where γ_R is the angle of reflection (see Figure 2). Then

$$\tan(\gamma_R) = \frac{c_2'}{c_1} = \frac{\tan(\gamma_I)}{1 + 2(\lambda_{12}^{(1)}/\lambda_{22}^{(1)})\tan(\gamma_I)} \tag{12}$$

and once γ_R has been determined from this equation, the wave speed β' of the reflected wave may be readily determined from the equation $\beta = c_1 \sin(\gamma_R)$.

To include the influence of a different anisotropic material in region 2 let the displacement in region 1 be given by (3) with

$$u^{(1)} = u_0^{(1)} + u_d^{(1)} \tag{13}$$

where $u_0^{(1)}$ denotes the displacement obtained from (7) while $u_d^{(1)}$ denotes the displacement due to diffracted waves. The displacement in region 2 is given by (3) with $u^{(2)} = u_r^{(2)}$ denoting the displacement associated with the refracted waves.

In order to find $u_d^{(1)}$ and $u_r^{(2)}$, it is convenient to obtain an integral equation solution of (4). To derive the integral equation, first consider the inhomogeneous equation associated with (4). That is,

$$\lambda_{ij}^{(\alpha)} \frac{\partial^2 u^{(\alpha)}}{\partial x_i \partial x_j} + \rho^{(\alpha)} \omega^2 u^{(\alpha)} = h^{(\alpha)}(x_1, x_2) \tag{14}$$

where $h^{(\alpha)}(x_1, x_2)$ is a given function. Any two solutions $U^{(\alpha)}$ and $V^{(\alpha)}$ of (14) are related by the integral equation

$$\int_{\partial\Omega} \left(\lambda_{ij}^{(\alpha)} \frac{\partial U^{(\alpha)}}{\partial x_j} n_i V \lambda^{(\alpha)} - \lambda_{ij}^{(\alpha)} \frac{\partial V^{(\alpha)}}{\partial x_j} n_i U^{(\alpha)} \right) ds = \int_{\Omega} \left(h_U^{(\alpha)} V^{(\alpha)} - h_V^{(\alpha)} U^{(\alpha)} \right) dv \tag{15}$$

where Ω is the region under consideration and Ω has a boundary $\partial\Omega$ with an outward pointing normal $\mathbf{n} = (n_1, n_2)$. Also $h_U^{(\alpha)}$ and $h_V^{(\alpha)}$ denote the

https://doi.org/10.1017/S0334270000007013 Published online by Cambridge University Press

right-hand side of (14) corresponding to the solutions $U^{(\alpha)}$ and $V^{(\alpha)}$ respectively.

Now suppose $h_V^{(\alpha)} = \delta(\mathbf{x} - \mathbf{x}_0)$ where δ denote the Dirac delta function, $\mathbf{x} = (x_1, x_2)$ and $\mathbf{x}_0 = (a, b)$ where $\mathbf{x} \in \Omega$ and $\mathbf{x}_0 \in \Omega$. Then if $u^{(\alpha)}(a, b) = U^{(\alpha)}$, (15) provides

$$Cu^{(\alpha)}(a, b) = \int_{\partial\Omega} \left[\lambda_{ij}^{(\alpha)} \frac{\partial V^{(\alpha)}}{\partial x_j} n_i u^{(\alpha)} - \lambda_{ij}^{(\alpha)} \frac{\partial u^{(\alpha)}}{\partial x_j} n_i V^{(\alpha)}\right] ds \qquad (16)$$

where C is a constant such that $C = 1$ if $(a, b) \in \Omega$ and if $(a, b) \in \partial\Omega$ then $0 < C < 1$. Also $V^{(\alpha)}$ satisfies the equation

$$\lambda_{ij}^{(\alpha)} \frac{\partial^2 V^{(\alpha)}}{\partial x_i \partial x_j} + \rho^{(\alpha)} \omega^2 V^{(\alpha)} = \delta(\mathbf{x} - \mathbf{x}_0). \qquad (17)$$

To obtain a solution to (16), it is helpful to proceed as follows. Let $z^{(\alpha)} = x_1 + \tau^{(\alpha)} x_2$ and $\overline{z}^{(\alpha)} = x_1 + \overline{\tau}^{(\alpha)} x_2$ where $\tau^{(\alpha)}$ is the complex root with positive imaginary part of the quadratic

$$\lambda_{11}^{(\alpha)} + 2\lambda_{12}^{(\alpha)} \tau^{(\alpha)} + \lambda_{22}^{(\alpha)} (\tau^{(\alpha)})^2 = 0 \qquad (18)$$

and the bar denotes the conjugate of a complex number. Then (17) transforms to

$$2\left[\lambda_{11}^{(\alpha)} + \lambda_{12}^{(\alpha)}(\tau^{(\alpha)} + \overline{\tau}^{(\alpha)}) + \tau^{(\alpha)}\overline{\tau}^{(\alpha)}\lambda_{22}^{(\alpha)}\right] \frac{\partial^2 V^{(\alpha)}}{\partial z^{(\alpha)} \partial \overline{z}^{(\alpha)}} + \rho^{(\alpha)} \omega^2 V^{(\alpha)} = \delta(\mathbf{x} - \mathbf{x}_0). \qquad (19)$$

Let $z^{(\alpha)} = \dot{x}_1^{(\alpha)} + \mathrm{i}\dot{x}_2^{(\alpha)}$, $\overline{z}^{(\alpha)} = \dot{x}_1^{(\alpha)} - \mathrm{i}\dot{x}_2^{(\alpha)}$ and $\tau^{(\alpha)} = \dot{\tau}^{(\alpha)} + \mathrm{i}\ddot{\tau}^{(\alpha)}$ where $\dot{x}_1^{(\alpha)}$, $\dot{x}_2^{(\alpha)}$, $\dot{\tau}^{(\alpha)}$ and $\ddot{\tau}^{(\alpha)}$ are real numbers. Then

$$\dot{x}_1^{(\alpha)} = x_1 + \dot{\tau}^{(\alpha)} x_2 \quad \text{and} \quad \dot{x}_2^{(\alpha)} = \ddot{\tau}^{(\alpha)} x_2. \qquad (20)$$

Use of (20) in (19) provides

$$\frac{\partial^2 V^{(\alpha)}}{\partial \dot{x}_1^2} + \frac{\partial^2 V^{(\alpha)}}{\partial \dot{x}_2^2} + \overline{\omega}^{(\alpha)^2} V^{(\alpha)} = K^{(\alpha)} \delta(\mathbf{x} - \mathbf{x}_0) \qquad (21)$$

where

$$\overline{\omega}^{(\alpha)^2} = \frac{2\omega^2 \rho^{(\alpha)}}{\lambda_{11}^{(\alpha)} + \lambda_{12}^{(\alpha)}(\tau^{(\alpha)} + \overline{\tau}^{(\alpha)}) + \tau^{(\alpha)}\overline{\tau}^{(\alpha)}\lambda_{22}^{(\alpha)}} \qquad (23)$$

and

$$K^{(\alpha)} = \frac{2}{\lambda_{11}^{(\alpha)} + \lambda_{12}^{(\alpha)}(\tau^{(\alpha)} + \overline{\tau}^{(\alpha)}) + \tau^{(\alpha)}\overline{\tau}^{(\alpha)}\lambda_{22}^{(\alpha)}}. \qquad (24)$$

A solution to (21) may be written in the form

$$V^{(\alpha)} = \frac{\mathrm{i}}{4} K^{(\alpha)} H_0^{(2)}(\overline{\omega}^{(\alpha)} R^{(\alpha)}) \qquad (25)$$

where $H_0^{(2)}$ denotes the Hankel function of the second kind and order zero and

$$R^{(\alpha)} = \sqrt{(\dot{x}_1^{(\alpha)} - \dot{a}^{(\alpha)})^2 + (\dot{x}_2^{(\alpha)} - \dot{b}^{(\alpha)})^2}, \tag{26}$$

where $\dot{a}^{(\alpha)} = a + \dot{\tau}^{(\alpha)} b$ and $\dot{b}^{(\alpha)} = b\ddot{\tau}^{(\alpha)}$ so that

$$R^{(\alpha)} = \sqrt{(x_1 + \dot{\tau}^{(\alpha)} x_2 - a - \dot{\tau}^{(\alpha)} b)^2 + (x_2 \ddot{\tau}^{(\alpha)} - b\ddot{\tau}^{(\alpha)})^2}. \tag{27}$$

Hence the integral equation is given by (16) with the fundamental solution $V^{(\alpha)}$ given by (25).

Now any solution to (17) may be used in the integral equation (16). Here it is convenient to choose a solution to (17) which gives rise to the term $\lambda_{2j}^{(\alpha)}(\partial V^{(\alpha)}/\partial x_j)$ equalling zero on $x_2 = 0$, it follows that the integral along the boundary $x_2 = 0$ in (16) will be zero. By image considerations it may be seen that a suitable choice of solution of (17) is

$$V^{(\alpha)} = \frac{\mathrm{i}}{4}\left[K^{(\alpha)} H_0^{(2)}(\overline{\omega}^{(\alpha)} R^{(\alpha)}) + K^{(\alpha)} H_0^{(2)}(\overline{\omega}^{(\alpha)} \overline{R}^{(\alpha)})\right], \tag{28}$$

where

$$R^{(\alpha)} = \sqrt{(x_1 + \dot{\tau}^{(\alpha)} x_2 - a - \dot{\tau}^{(\alpha)} b)^2 + (x_2 \ddot{\tau}^{(\alpha)} - b\ddot{\tau}^{(\alpha)})^2} \tag{29}$$

and

$$\overline{R}^{(\alpha)} = \sqrt{(x_1 + \dot{\tau}^{(\alpha)} x_2 - a - \dot{\tau}^{(\alpha)} b)^2 + (x_2 \ddot{\tau}^{(\alpha)} + b\ddot{\tau}^{(\alpha)})^2}. \tag{30}$$

By applying (16) to region 1 with the Green's function (28) it is only necessary to integrate over the material interface between regions 1 and 2. The integration along the Ox_1 axis is zero so the only contribution is obtained from the interface. Similarly in region 2 it is necessary to integrate only on the interface between regions 1 and 2. In applying the integral equation (16), the boundary conditions over the interface involve the continuity of stress and displacement so that

$$u^{(1)} = u^{(2)}, \tag{31}$$

and

$$\begin{aligned}\left(\lambda_{11}^{(1)}\frac{\partial u^{(1)}}{\partial x_1} + \lambda_{12}^{(1)}\frac{\partial u^{(1)}}{\partial x_2}\right) n_1 + \left(\lambda_{21}^{(1)}\frac{\partial u^{(1)}}{\partial x_1} + \lambda_{22}^{(1)}\frac{\partial u^{(1)}}{\partial x_2}\right) n_2 \\ = \left(\lambda_{11}^{(2)}\frac{\partial u^{(2)}}{\partial x_1} + \lambda_{12}^{(2)}\frac{\partial u^{(2)}}{\partial x_2}\right) n_1 + \left(\lambda_{21}^{(2)}\frac{\partial u^{(2)}}{\partial x_1} + \lambda_{22}^{(2)}\frac{\partial u^{(2)}}{\partial x_2}\right) n_2.\end{aligned} \tag{32}$$

The conditions (31) and (32) can be used in conjunction with (16) to solve for the displacement and stress over the interface and the displacement along

https://doi.org/10.1017/S0334270000007013 Published online by Cambridge University Press

the traction free surface $x_2 = 0$. Once this has been done, (16) gives the value of $u^{(\alpha)}(a, b)$ at all points (a, b) in the half-space $x_2 > 0$.

4. Numerical results

Suppose region 2 (Figure 1) is defined by $x_1^2 + x_2^2 \leq a^2$ with $x_2 \geq 0$, the material in region 1 has the elastic moduli $\lambda_{ij}^{(1)}$ and density $\rho^{(1)}$ and the material in region 2 has the elastic moduli $\lambda_{ij}^{(2)}$ and density $\rho^{(2)}$.

The material properties can be written as dimensionless quantities in the form

$$\dot{\lambda}_{ij}^{(\alpha)} = \lambda_{ij}^{(\alpha)} / \lambda_{11}^{(1)} \tag{33}$$

and

$$\rho = \rho^{(2)} / \rho^{(1)}. \tag{34}$$

The ratio of the diameter $2a$ of the alluvial valley to the wavelength Λ of the incident wave is denoted by η so that

$$\eta = 2a/\Lambda. \tag{35}$$

Let T be the duration of time for the initial wave to travel a distance of one wave length Λ so that

$$T = \Lambda/\beta^{(1)} \tag{36}$$

or from (1)

$$T = 2\pi/\omega. \tag{37}$$

Use of (35), (36) and (37) provides

$$\omega = \eta\pi\beta^{(1)}/a. \tag{38}$$

All length measurements are made dimensionless by referring lengths to the valley's radius a. So $x_1' = x_1/a$ and $x_2' = x_2/a$. Using these dimensionless quantities, (16) becomes

$$Cu^{(\alpha)}(c, d) = \int_{\partial\Omega} \left[\dot{\lambda}_{ij}^{(\alpha)} \frac{\partial \dot{V}^{(\alpha)}}{\partial x_j'} n_i u^{(\alpha)} - \dot{\lambda}_{ij}^{(\alpha)} \frac{\partial u^{(\alpha)}}{\partial x_j'} n_i \dot{V}^{(\alpha)} \right] ds \tag{39}$$

https://doi.org/10.1017/S0334270000007013 Published online by Cambridge University Press

where

$$\dot{V}^{(\alpha)} = \frac{\mathrm{i}}{4}\left[\dot{K}^{(\alpha)} H_0^{(2)}(\dot{\omega}^{(\alpha)}\dot{R}^{(\alpha)}) + \dot{K}^{(\alpha)} H_0^{(2)}(\omega^{(\alpha)}\overline{\dot{R}}^{(\alpha)})\right], \tag{40}$$

$$\dot{R}^{(\alpha)} = \sqrt{(x_1' + \dot{\tau}^{(\alpha)}x_2' - c' - \dot{\tau}^{(\alpha)}\,d')^2 + (x_2'\ddot{\tau}^{(\alpha)} - d'\ddot{\tau}^{(\alpha)})^2}, \tag{41}$$

$$\overline{\dot{R}}^{(\alpha)} = \sqrt{(x_1' + \dot{\tau}^{(\alpha)}x_2' - c' - \dot{\tau}^{(\alpha)}\,d')^2 + (x_2'\ddot{\tau}^{(\alpha)} + d'\ddot{\tau}^{(\alpha)})^2}, \tag{42}$$

$$\dot{K}^{(\alpha)} = \frac{2}{(\dot{\lambda}_{11}^{(\alpha)} + 2\dot{\lambda}_{12}^{(\alpha)}\dot{\tau}^{(\alpha)} + ([\dot{\tau}^{(\alpha)}]^2 + [\ddot{\tau}^{(\alpha)}])^2\dot{\lambda}_{22}^{(\alpha)})}, \tag{43}$$

$$[\dot{\omega}^{(1)}]^2 = \dot{K}^{(1)}[\pi\eta\dot{\beta}^{(1)}]^2, \tag{44}$$

$$[\dot{\omega}^{(2)}]^2 = \dot{K}^{(2)}\rho[\pi\eta\dot{\beta}^{(1)}]^2, \tag{45}$$

$$[\dot{\beta}^{(1)}]^2 = \dot{\lambda}_{11}^{(1)}\sin^2\gamma_I + 2\dot{\lambda}_{12}^{(1)}\sin\gamma_I\cos\gamma_I + \dot{\lambda}_{22}^{(1)}\cos^2\gamma_I, \tag{46}$$

$$\dot{\tau}^{(\alpha)} = \dot{\lambda}_{12}^{(\alpha)}/\dot{\lambda}_{22}^{(\alpha)}, \tag{47}$$

and

$$\left[\ddot{\tau}^{(\alpha)}\right]^2 = \left(\frac{\dot{\lambda}_{11}^{(\alpha)}}{\dot{\lambda}_{22}^{(\alpha)}} - \left(\frac{\dot{\lambda}_{12}^{(\alpha)}}{\dot{\lambda}_{22}^{(\alpha)}}\right)^2\right). \tag{48}$$

The displacement $u^{(\alpha)}(c, d)$ has amplitude χ which is the ratio of the displacement to the amplitude of the initial incident wave $u_i^{(\alpha)}$.

Since the initial incident wave has amplitude unity it follows that the displacement can be written as

$$u^{(\alpha)} = \chi\exp(\mathrm{i}\phi). \tag{49}$$

In the numerical calculations, values of the displacement amplitude χ were obtained on the surface $x_2' = 0$, which is the place of interest in most considerations concerning earthquakes. The amplitude χ is a function of the parameters η, ρ, γ_I, and the moduli $\dot{\lambda}_{ij}^{(\alpha)}$.

If the material in either region 1 or region 2 is transversely isotropic and the x_1^* and x_2^* axes are the axes of symmetry for the material with the x_3 axis normal to the transverse plane, then using the transformation law for Cartesian tensors

$$\dot{\lambda}_{ij}^{(\alpha)} = a_{im}a_{jn}\dot{\lambda}_{mn}^{*(\alpha)} \tag{50}$$

where $\dot{\lambda}_{11}^{*(\alpha)}$, $\dot{\lambda}_{22}^{*(\alpha)}$ and $\dot{\lambda}_{12}^{*(\alpha)} = 0$ are the elastic moduli referred to the $Ox_1^*x_2^*$ frame and

$$(a_{ij}) = \begin{pmatrix} \cos(\zeta) & \sin(\zeta) \\ -\sin(\zeta) & \cos(\zeta) \end{pmatrix} \tag{51}$$

where ζ is the angle between the x_1^* axis and the x_1 axis (Figure 3).

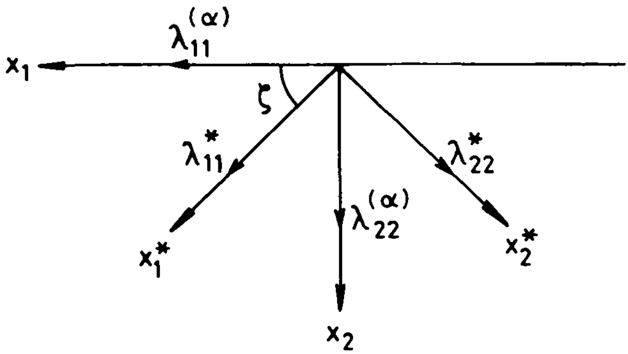

FIGURE 3. Angle of anisotropy ζ.

The numerical procedure used to solve the boundary integral equation (16) was a standard procedure used for equations of this type [4]. The interface boundary between regions 1 and 2 was divided into 80 equal segments and the unknowns in (16) assumed to be constant over each segment. Equation (16) was thus reduced to a system of linear algebraic equations for the values of the unknown variables on each segment. Once this system was solved, (16) was used to determine the displacement on the line $x_2 = 0$. Results for the case when both regions 1 and 2 are isotropic compared favourably with the results published in [6]. Further results for the isotropic case compared well with values calculated by the method published in [7].

The numerical solutions displayed in Figures 4, 5, 6, 7 and 8 are for the case when region 1 is an isotropic material with $\dot{\lambda}_{11}^{(1)} = 1$, $\dot{\lambda}_{22}^{(1)} = 1$, $\dot{\lambda}_{12}^{(1)} = 0$ and $\rho = 2/3$. For Figures 4, 5 and 6, region 2 has the parameters $\dot{\lambda}_{11}^{*(2)} = 1/6$,

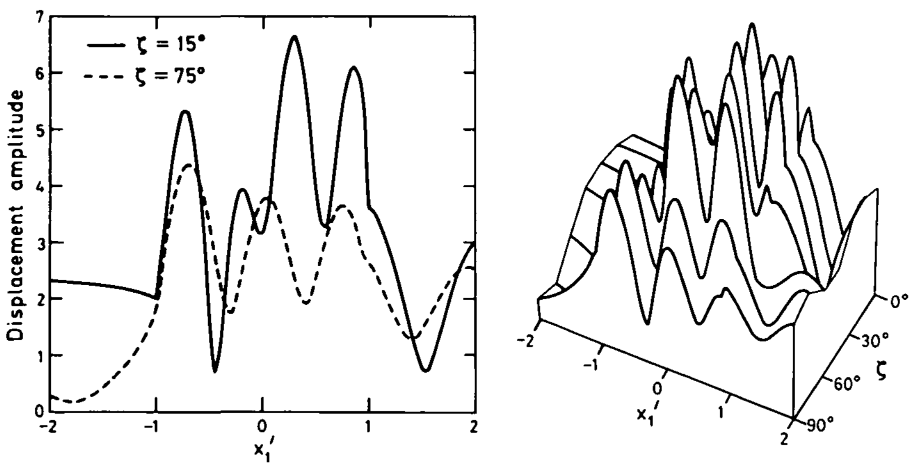

FIGURE 4. Effect of anisotropy, $\gamma_I = 60°$.

https://doi.org/10.1017/S0334270000007013 Published online by Cambridge University Press

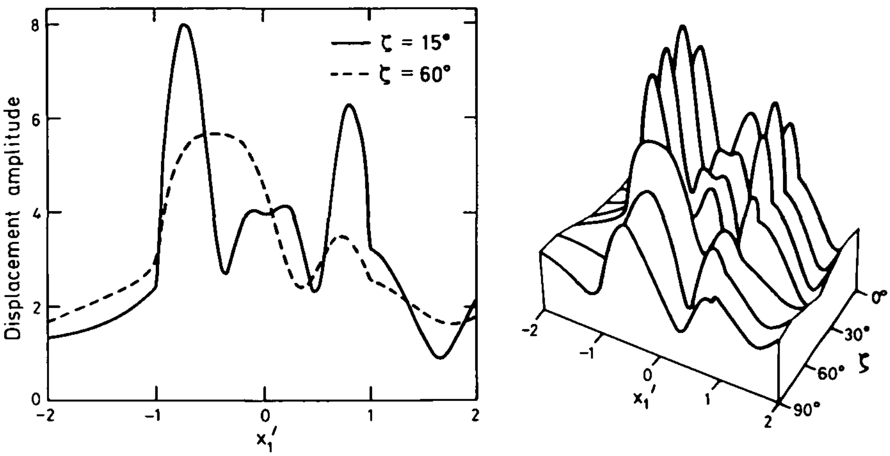

FIGURE 5. Effect of anisotropy, $\gamma_I = 30^\circ$.

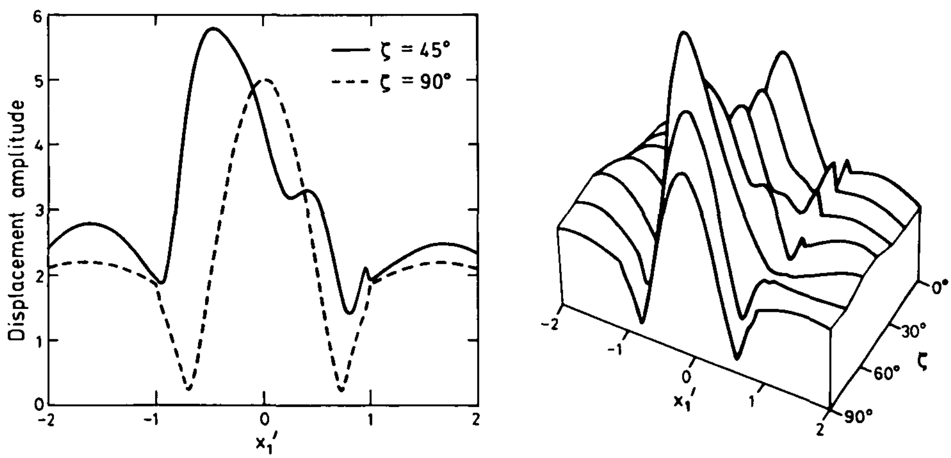

FIGURE 6. Effect of anisotropy, $\gamma_I = 0^\circ$.

$\dot{\lambda}_{22}^{*(2)} = 1/3$, $\dot{\lambda}_{12}^{*(2)} = 0$ and $\eta = 1.0$. Calculations were carried out for the angles $\zeta = 0^\circ$, 15°, 30°, 45°, 60°, 75° and 90°. In Figure 4, $\gamma_I = 60^\circ$, while in Figure 5, $\gamma_I = 30^\circ$ and in Figure 6, $\gamma_I = 0^\circ$. These figures illustrate the effect of anisotropy in the alluvial valley on the surface displacements.

The results show how anisotropy effects the location of the largest displacement amplitude. For example, it is clear from Figure 6 that when $\zeta = 0^\circ$ and 90°, the displacement is symmetric about $x_1' = 0$ but when $0 < \zeta < 90$, the maximum displacement lies in the region $-2 < x_1' < 0$.

Results shown in Figure 7 are for the same parameters as Figure 4 with $\gamma_I = 60^\circ$, but with the semi-circular geometry in region 2 replaced by a

https://doi.org/10.1017/S0334270000007013 Published online by Cambridge University Press

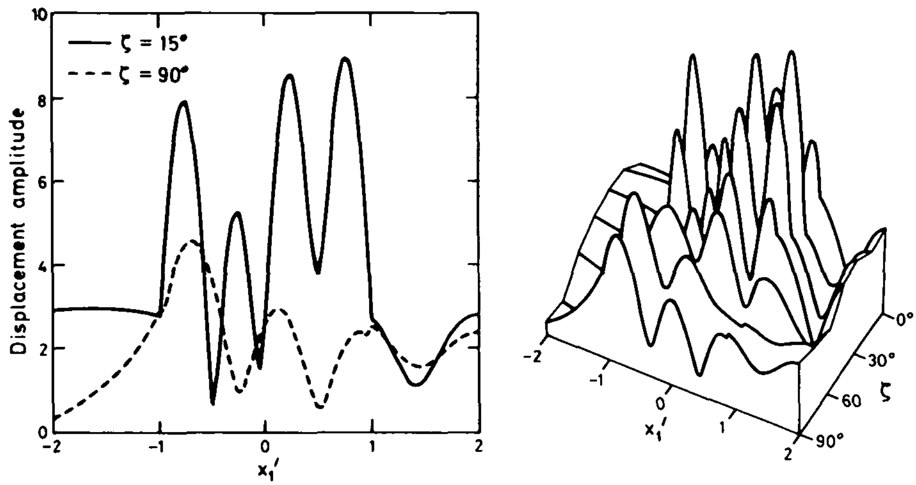

FIGURE 7. Effect of a rectangular valley.

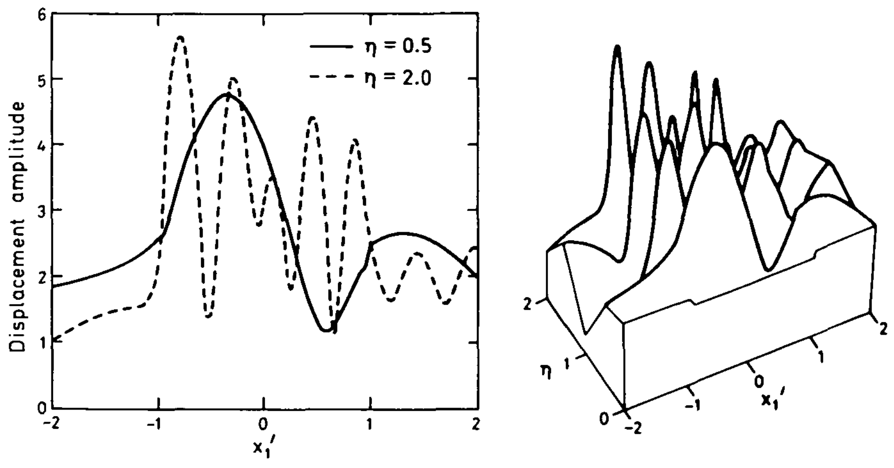

FIGURE 8. Effect of wavelength.

rectangle with length $2a$ along the x_1 axis and depth a on the x_2 axis.

Figure 8 shows results obtained using the same parameters as in Figure 4 but with $\zeta = 75^\circ$ and $\eta = 0.1$, 0.5, 1.0, 1.5, 2.0. The results show that in this case, the number of peaks and troughs in the displacement amplitude varied significantly for different wavelenghts.

In Figure 9, anisotropy was introduced to the surrounding material in region 1. The alluvial valley had the same parameters as for Figure 7 but the outside material had the elastic moduli $\dot{\lambda}_{11}^{*(1)} = 1/6$, $\dot{\lambda}_{22}^{*(1)} = 1/3$ and $\eta = 1.0$. The angle ζ was varied in steps of 15° and the results showed that

https://doi.org/10.1017/S0334270000007013 Published online by Cambridge University Press

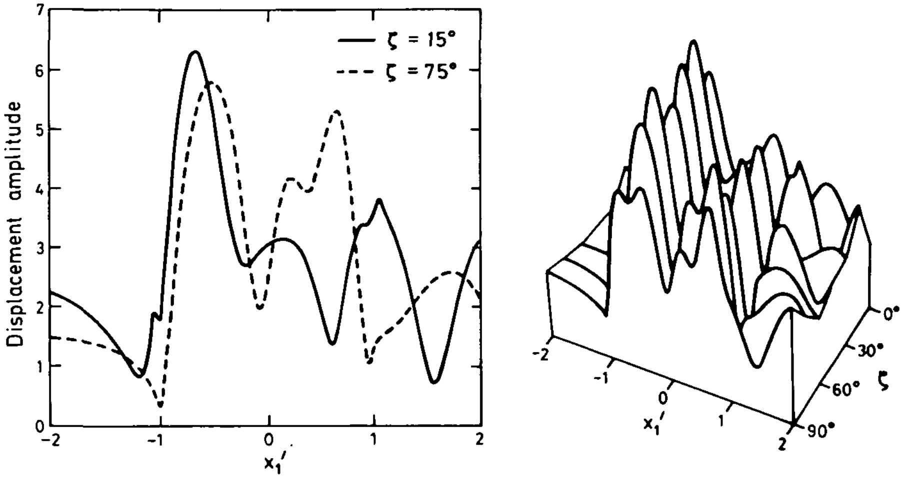

FIGURE 9. Effect of anisotropy in region 1.

the angle ζ for region 1 had little effect on the displacement amplitude on the surface in region 2.

5. Conclusion

A boundary element method for the scattering and diffraction of SH waves by anisotropic alluvial valleys with an arbitrary cross section has been constructed in this paper by the use of the fundamental solution given in (28). The use of (16) allows the surface displacement to be calculated. The method includes previously obtained methods as special cases. For these cases the numerical results compared well with those given by Trifunac's method and by Sanchez-Sesma and Esquivel [6].

For the materials considered in numerical examples the results showed that anisotropy in the valley has a significant effect on the amplitude of the surface displacement.

References

[1] K. Aki and K. L. Larner, "Surface motion of a layered medium having an irregular interface due to incident plane SH waves", *J. Geophys. Res.* **75** (1970) 933–954.

[2] D. M. Boore, "A note on the effect of simple topography on seismic SH waves", *Bull. Seism. Soc. Am.* **72** (1972) 275–284.

[3] M. Bouchon, "Effect of topography on surface motion", *Bull. Seism. Soc. Am.* **63** (1973) 715–732.

[4] D. Clements, *Boundary value problems governed by second order elliptic systems* (Pitman, 1983).

[5] D. E. Hudson, "Local distribution of strong earthquake motion", *Bull. Seism. Soc. Am.* **62** (1972) 1765–1786.
[6] F. J. Sánchez-Sesma and J. A. Esquivel, "Ground motion on alluvial valleys under incident plane SH waves", *Bull. Seis. Soc. Am.* **69** (1979) 1107–1120.
[7] M. D. Trifunac, "Surface motion of a semi-cylindrical alluvial valley for incident plane SH-waves", *Bull. Seism. Soc. Am.* **61** (1971) 1755–1770.
[8] M. D. Trifunac, "Scattering of plane SH waves by a semi-cylindrical canyon", *Intern. J. Earthquake Eng. Struct. Dyn.* **1** (1973) 267–281.
[9] H. L. Wong and P. C. Jennings, "Effects of canyon topography on strong ground motion", *Bull. Seism. Soc. Am.* **65** (1975) 1239–1258.
[10] H. L. Wong and M. D. Trifunac, "Surface motion of a semi-elliptical alluvial valley for incident plane SH waves", *Bull Seism. Soc. Am.* **64** (1974) 1389–1408.
[11] H. L. Wong, M. D. Trifunac and B. Westermo, "Effects of surface and subsurface irregularities on the amplitudes of monochromatic waves", *Bull. Seism. Soc. Am.* **67** (1977) 353–368.